This study is the basis for further work that will probe the effect of solvent on the reaction and the effect of changing the electron-transfer distance through study of derivatives of the cobalt complex and ferrocene.

Acknowledgment is made to the donors of the Petroleum Research Fund, administered by the American Chemical Society, the M. J. Murdock Charitable Trust of the Research Corp., and the Washington State University Grant in Aid program for support of this research.

Registry No. $Fe(cp)_2$, 102-54-5; $Co(dmg)_3(BF)_2BF_4$, 34248-48-1; n-Bu_4NBF_4, 429-42-5.

Supplementary Material Available: Tables of kinetic and thermodynamic data (5 pages). Ordering information is given on any current masthead page.

Contribution from the Department of Chemistry,
Texas A&M University, College Station, Texas 77843

Tris(2,2'-bipyridine)ruthenium(III) in Zeolite Y: Characterization and Reduction on Exposure to Water

WILLIAM H. QUAYLE and JACK H. LUNSFORD*

Received March 5, 1981

A $[Ru^{III}(bpy)_3]$-Y zeolite containing 2.1 wt % Ru was reduced by water at 70 °C to $[Ru^{II}(bpy)_3]$-Y; however, dioxygen was not a product of the reaction. The immobility of the Ru(III) complex in the zeolite, as well as an unfavorable local chemical environment, probably inhibits the secondary electron-transfer processes necessary for O_2 formation. The $[Ru^{III}(bpy)_3]$-Y zeolite was prepared by exposure of $[Ru^{II}(bpy)_3]$-Y to chlorine gas. The low-spin d^5 complex was characterized by EPR ($g_\perp = -2.67$, $g_\parallel = 1.24$) and visible diffuse-reflectance (λ_{max} = 685 and 420 nm) spectroscopies. XRD and XPS studies confirm that the complex in the original $[Ru^{II}(bpy)_3]$-Y material was intrazeolitic.

Introduction

We have shown recently that tris(2,2'-bipyridine)ruthenium(II) complex cations are formed within the cavities of Y type zeolites when 2,2'-bipyridine (bpy) is mixed and heated with Ru^{III}-Y zeolites.[1] The spectroscopic properties of these $[Ru^{II}(bpy)_3]$-Y zeolites were similar to those exhibited by $[Ru^{II}(bpy)_3]^{2+}$ complexes in aqueous solution. The zeolite complexes, however, displayed anomalous variability in their photophysical behavior, which was dependent upon the extent of hydration and the degree of complex loading within the zeolite. These preliminary studies indicated the importance of detailed consideration of the effects of ligand and chemical environments on the photophysics and therefore their effects on the photoreactivities of transition-metal complexes. This study also indicated that zeolites might be attractive supports within which the environments of transition-metal complexes could be selectively altered to enhance desired photoreactions and photocatalytic processes. An interest in the redox and photochemical properties of transition-metal complexes in zeolites prompted us to examine the oxidation of degassed $[Ru^{II}(bpy)_3]$-Y to $[Ru^{III}(bpy)_3]$-Y by chlorine gas and the subsequent reduction of $[Ru^{III}(bpy)_3]$-Y by H_2O.

The oxidation of water by $[Ru^{III}(bpy)_3]^{3+}$ salts has been known for some time. Dwyer and Gyarfas[2] detected ozone and H_2O_2 formation on dissolution of tris(bipyridine) salts of Fe(III), Ru(III), and Os(III) in water. Creutz and Sutin[3] investigated the kinetics of the reaction of hydroxide ion with the Ru(III) complex (eq 1) and discussed the potential use

$$[Ru^{III}(bpy)_3]^{3+} + OH^- \rightarrow [Ru^{II}(bpy)_3]^{2+} + {}^1/_4O_2 + {}^1/_2H_2O \quad (1)$$

of this reaction for the photocatalytic splitting of water (eq 2). The successful coupling of eq 1, or analogous reactions,

$$H_2O \xrightarrow[cat]{h\nu} H_2 + {}^1/_2O_2 \quad (2)$$

with either photoassisted water-reduction processes[4-13] or other $[Ru^{III}(bpy)_3]^{3+}$ initiated water-oxidation reactions,[14-17] has resulted in potentially attractive solar energy storage systems.

Results and Discussion

$[Ru^{II}(bpy)_3]$-Y. The visible-region diffuse-reflectance spectrum of the degassed (>95% of the intrazeolitic H_2O removed[1]) synthesized $[Ru^{II}(bpy)_3]$-Y sample containing 2.1 wt % Ru is shown in Figure 1, curve a. It exhibits the λ_{max} = 450 nm absorption band characteristic of orange $[Ru^{II}(bpy)_3]^{2+}$ complexes.[18] In our preliminary studies,[1] synthesized $[Ru^{II}(bpy)_3]$-Y zeolites were prepared by mixing bpy with a $[Ru^{III}(NH_3)_6]$-Y zeolite in a 4:1 bpy:Ru mole ratio. Our initial employment of the 4:1 ratio was based on the stoichiometry of Burstall's[19] original preparation of $[Ru^{II}(bpy)_3]Cl_2$ (eq 3). We have since found that 3:1 or preferably

$$2Ru^{3+} + 8bpy \xrightarrow{200\ °C} 2[Ru^{II}(bpy)_3]^{2+} + C_{20}H_{14}N_4 + 2H^+ \quad (3)$$

3.5:1 mole ratios of bpy:Ru also form $[Ru^{II}(bpy)_3]$-Y. Intrazeolitic ammonia was probably the ruthenium-reducing

(1) DeWilde, W.; Peeters, G.; Lunsford, J. H. *J. Phys. Chem.* **1980**, *84*, 2306.
(2) Dwyer, F. P.; Gyarfas, E. C. *J. Am. Chem. Soc.* **1952**, *74*, 4669.
(3) Creutz, C.; Sutin, N. *Proc. Natl. Acad. Sci. U.S.A.* **1975**, *72*, 2858.
(4) Kiwi, J.; Borgarello, E.; Pelizzetti, E.; Visca, M.; Grätzel, M. *Angew. Chem., Int. Ed. Engl.* **1980**, *19*, 647.
(5) Kalyanasundaram, K.; Grätzel, M. *Angew. Chem., Int. Ed. Engl.* **1979**, *18*, 701.
(6) Kalyanasundaram, K.; Kiwi, J.; Grätzel, M. *Helv. Chim. Acta* **1978**, *61*, 2720.
(7) Ryason, P. R. U.S. Patent 4 105 517, 1978.
(8) Keller, P.; Moradpour, A.; Amouyal, E.; Kagan, H. B. *Nouv. J. Chim.* **1980**, *4*, 377.
(9) Brown, G. M.; Brunschwig, B. S.; Creutz, C.; Endicott, J. F.; Sutin, N. *J. Am. Chem. Soc.* **1979**, *101*, 1298.
(10) Gohn, M.; Getoff, N. *Z. Naturforsch., A* **1979**, *34A*, 1135.
(11) Okura, I.; Kim-Thuan, N. *J. Mol. Catal.* **1979**, *5*, 311.
(12) Lehn, J.-M.; Sauvage, J.-P. *Nouv. J. Chim.* **1977**, *1*, 449.
(13) Neumann-Spallart, M.; Kalyanasundaram, K.; Grätzel, C.; Grätzel, M. *Helv. Chim. Acta* **1980**, *63*, 1111.
(14) Shafirovich, V. Ya.; Khannanov, N. K.; Strelets, V. V. *Nouv. J. Chim.* **1980**, *4*, 81.
(15) Lehn, J.-M.; Sauvage, J.-P.; Ziessel, R. *Nouv. J. Chim.* **1979**, *3*, 423.
(16) Shafirovich, V. Ya.; Shilov, A. E. *Kinet. Katal.* **1979**, *20*, 1156.
(17) Lehn, J.-M.; Sauvage, J.-P.; Ziessel, R. *Nouv. J. Chim.* **1980**, *4*, 355.
(18) Palmer, R. A.; Piper, T. S. *Inorg. Chem.* **1966**, *5*, 864.
(19) Burstall, F. H. *J. Chem. Soc.* **1936**, 173.

0020-1669/82/1321-0097$01.25/0

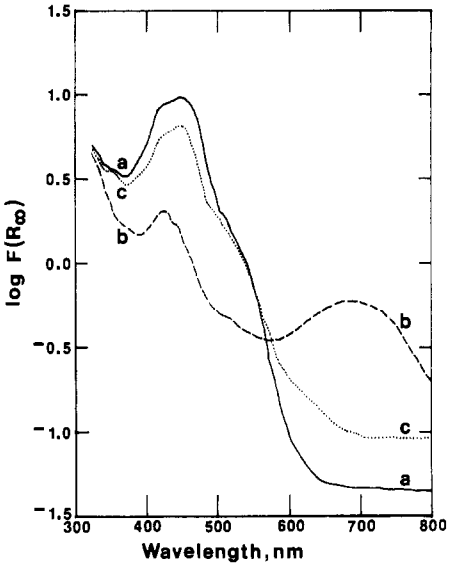

Figure 1. Visible-region diffuse-reflectance spectra: (a) outgassed, 2.1 wt % Ru, $[Ru^{II}(bpy)_3]Y$; (b) outgassed 2.1 wt % Ru, $[Ru^{III}(bpy)_3]Y$; (c) sample b, after exposure to water.

agent in the absence of excess bpy in these latter cases. As a consequence, eq 4 and 5 may have contributed to $[Ru^{II}(bpy)_3]$–Y formation in addition to eq 3. These reactions are quite plausible in view of recent observations that, upon heating in the absence of O_2, $[Ru^{III}(NH_3)_6]$–Y zeolites undergo self-reduction with concomitant formation of N_2.[20,21]

$$2[Ru^{III}(NH_3)_6]^{3+} + 6bpy \xrightarrow{200\ °C} 2[Ru^{II}(bpy)_3]^{2+} + N_2H_4 + 2NH_4^+ + 8NH_3 \quad (4)$$

$$6[Ru^{III}(NH_3)_6]^{3+} + 18bpy \xrightarrow{200\ °C} 6[Ru^{II}(bpy)_3]^{2+} + N_2 + 6NH_4^+ + 28NH_3 \quad (5)$$

It was not possible to ion exchange $[Ru^{II}(bpy)_3]^{2+}$ directly within Y type zeolites, unlike layer-lattice silicates.[22-24] The diameter of the complex (~1.08 nm[25]) is too large for effective penetration through the zeolite-lattice free apertures (~0.74 nm[26]), but it should be small enough to fit once the complex is formed in the large cavities (free internal diameter ~1.3 nm[26]). An impregnated material was prepared by mixing a solution of $[Ru^{II}(bpy)_3]Cl_2$ with a Na–Y zeolite, followed by vacuum evaporation of solvent water.

Portions of X-ray powder diffraction (XRD) patterns for samples of (a) Na–Y, (b) 2.0 wt % Ru, impregnated $[Ru^{II}(bpy)_3]$–Y, and (c) 2.1 wt % Ru, synthesized $[Ru^{II}(bpy)_3]$–Y used in this study are reproduced in Figure 2. There was no appreciable loss in zeolite crystallinity for either the impregnated or synthesized $[Ru^{II}(bpy)_3]$–Y samples compared to the NaY. The lines in pattern b of Figure 2 marked with asterisks correspond to *d* values of 1.075 and 1.148 nm. These lines do not arise from the zeolite lattice but probably arise from $[Ru^{II}(bpy)_3]Cl_2$ crystallites that either precipitated with or adsorbed on the zeolite during the impregnation process. The XRD pattern of a sample of $[Ru^{II}(bpy)_3]Cl_2 \cdot xH_2O$ prepared in our laboratory (not shown) also exhibits lines with these *d* values.

Table I. Selected Binding Energies (eV) for Crystalline, Impregnated and Synthesized $[Ru^{II}(bpy)_3]^{2+}$ Samples[a]

state	$[Ru^{II}(bpy)_3]$-$Cl_2 \cdot xH_2O$	$[Ru^{II}(bpy)_3]Y$	
		imp[b]	syn[c]
Ru $3d_{5/2}$	281.6	281.8	281.3
Ru $3d_{3/2}$	286.7	287.4	287.1
Ru $3p_{3/2}$	463.6	463.6	463.3
N 1s	400.9	401.1	400.7
Si 2s		154.0	154.0
Si 2p		103.0	102.9
Al 2p		74.8	74.5

[a] All values ±0.2 eV and normalized to Si 2s = 154.0 eV. $[Ru^{II}(bpy)_3]Cl_2 \cdot xH_2O$ values normalized to an average C 1s value of 285.7 eV. [b] 2.0 wt % Ru. [c] 2.1 wt % Ru.

Table II. Surface Concentration Ratios for Impregnated, Synthesized, and Crystalline $[Ru^{II}(bpy)_3]^{2+}$ Samples[a]

state ratios	$[Ru^{II}(bpy)^3]Y$			$[Ru^{II}(bpy)_3]$-$Cl_2 \cdot xH_2O$
	imp[b]		syn[c]	
Ru $3d_{5/2}$/Al 2p	0.087	(0.06)[d]	0.030	
Ru $3p_{3/2}$/Al 2p	0.081		0.040	
(N 1s/Al 2p)/6	0.107		0.052	
Ru $3d_{5/2}$/Si 2p	0.032	(0.02)	0.010	
Ru $3p_{3/2}$/Si 2p	0.029		0.014	
(N 1s/Si 2p)/6	0.039		0.018	
N 1s/Ru $3d_{5/2}$	7.35	(6.00)	10.5	8.71
N 1s/Ru $3p_{3/2}$	7.90		7.89	8.55
Ru $3p_{3/2}$/Ru $3d_{5/2}$	0.93	(1.00)	1.33	1.02
Si 2p/Al 2p	2.77	(2.53)	2.91	

[a] Corrected concentration ratios determined by $n_1/n_2 = I_1\sigma_2/I_2\sigma_1$. [b] 2.0 wt % Ru. [c] 2.1 wt % Ru. [d] Bulk analysis values in parentheses.

It has been observed that an empirically derived relationship exists between the relative 331, 311, and 220 XRD pattern peak intensities and cation location in faujasite type zeolites.[27] Cations are randomly distributed within the lattice if $I_{331} > I_{220} > I_{311}$, but if $I_{331} > I_{311} > I_{220}$, the cations assume positions at sites II and I′. It may be seen from Figure 2, patterns a and b, that little change occurred in the relative intensities of the 331, 311, and 220 peaks upon impregnation of the NaY with $[Ru^{II}(bpy)_3]^{2+}$. Retention of random sodium ion location within the lattice is thus assumed. However, analysis of the pattern for the synthesized $[Ru^{II}(bpy)_3]$–Y sample indicates that significant cation redistribution occurred following complex formation. We presume that this is an indication that the large $[Ru^{II}(bpy)_3]^{2+}$ complexes displaced sodium ions from their random positions in the supercages to locations at sites I′ and II. This displacement should not be perceived as having occurred in each supercage, since the 2.1 wt % Ru loading would correspond only to about 1 complex per 2.3 supercages.

A previous determination that the location of the complex was within the zeolite lattice was made by a qualitative technique involving X-ray photoelectron spectroscopy (XPS).[1] Comparison of the signal intensities of the Ru $3d_{5/2}$ lines for a synthesized $[Ru^{II}(bpy)_3]$–Y sample and an impregnated sample indicated that the latter had a higher surface complex concentration than the former despite the former's higher total complex content. These XPS experiments were repeated and expanded to include concentration ratios for the complex relative to the aluminum or silicon of the zeolite lattice. This

(20) Elliott, D. J.; Lunsford, J. H. *J. Catal.* **1979**, *57*, 11.
(21) Pearce, J. R.; Mortier, W. J.; Uytterhoeven, J. B. *J. Chem. Soc., Faraday Trans. 1* **1979**, *75*, 1395.
(22) Traynor, M. F.; Mortland, M. M.; Pinnavaia, T. J. *Clays Clay Miner.* **1978**, *26*, 318.
(23) Schoonheydt, R. A.; Pelgrims, J.; Heroes, Y.; Uytterhoeven, J. B. *Clay Miner.* **1978**, *13*, 435.
(24) Krenske, D.; Abdo, S.; Van Damme, H.; Cruz, M.; Fripiat, J. J. *J. Phys. Chem.* **1980**, *84*, 2447.
(25) Rillema, D. P.; Jones, D. S.; Levy, H. A. *J. Chem. Soc., Chem. Commun.* **1979**, 849.
(26) Breck, D. W. "Zeolite Molecular Sieves"; Wiley: New York, 1974; p 177.
(27) Pearce, J. R., unpublished results.

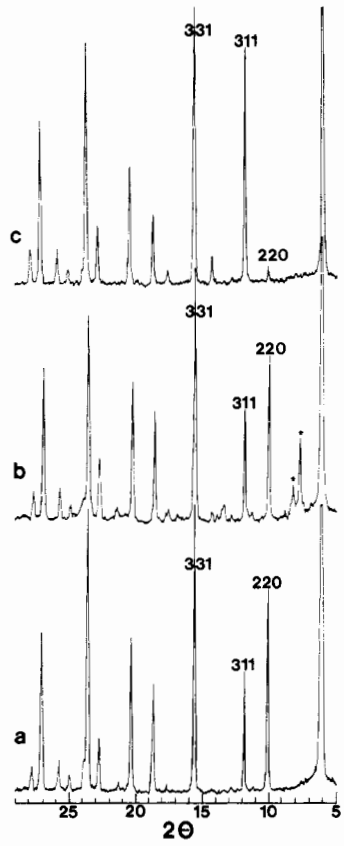

Figure 2. X-ray powder diffraction patterns: (a) NaY; (b) impregnated, 2.0 wt % Ru, $[Ru^{II}(bpy)_3]Y$; (c) synthesized, 2.1 wt % Ru, $[Ru^{II}(bpy)_3]Y$.

allowed a more reliable confirmation of intrazeolitic complex location.

Table I lists the binding energies determined for the Ru $3d_{5/2}$, Ru $3d_{3/2}$, Ru $3p_{3/2}$, and N 1s electrons of the $[Ru^{II}(bpy)_3]^{2+}$ samples. Significantly, the respective states exhibit similar binding energies, within experimental error (±0.2 eV), for each of the three different complex environments. Comparison of the corrected surface concentration ratios listed in Table II for the impregnated and synthesized $[Ru^{II}(bpy)_3]$–Y samples indicates that the impregnated material definitely possessed higher external surface complex content, despite the near equivalence in Ru loading of the two samples. The observed Ru/Al and Ru/Si ratios are up to 50% less than the ratios of ~0.06 and ~0.02, respectively, based on chemical analysis. These unexpectedly small ratios are fairly typical for metal ions in zeolites,[28] and they may reflect differences in escape depth of exiting electrons, depletion of aluminum and therefore exchange sites near the surface, errors in the cross sections, and in the case of Ru $3d_{5/2}$, errors due to overlap with the C 1s line. The latter error apparently is also responsible for the unusually large N 1s/Ru $3d_{5/2}$ ratio of 10.5 in the synthesized $[Ru^{II}(bpy)_3]$–Y complex. The other N/Ru ratios are reasonably constant and fall between the experimental values of the pure complex and the theoretical ratios based on the formula of the complex.

$[Ru^{III}(bpy)_3]$–Y. Oxidation of degassed, 2.1 wt % Ru, synthesized $[Ru^{II}(bpy)_3]$–Y by chlorine gas yielded a light green $[Ru^{III}(bpy)_3]$–Y sample. The visible diffuse-reflectance spectrum of the degassed material, Figure 1, curve b, exhibits absorption maxima at 685 and 420 nm (lit.[29] 680 and 418 nm).

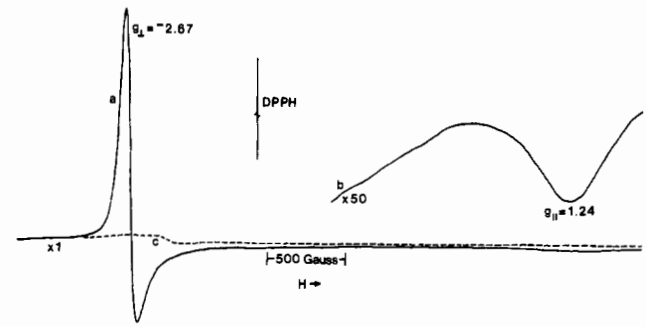

Figure 3. Electron paramagnetic resonance spectra taken at −196 °C: (a) 2.1 wt % Ru, $[Ru^{III}(bpy)_3]Y$; (b) sample a, at 50× greater receiver gain; (c) sample a, following exposure to water and outgassing.

Table III. EPR Data for Ru(III) Samples

	$[Ru^{III}(bpy)_3](PF_6)_3$[a]	$[Ru^{III}(bpy)_3]Y$
$g_\perp$	−2.64 ± 0.02	−2.67 ± 0.02
$g_\parallel$	1.14 ± 0.03	1.24 ± 0.01
k	0.932 ± 0.03[b]	0.981 ± 0.03[b]
ν/ξ	1.91 ± 0.05[b]	2.08 ± 0.03[b]

[a] $[Ru^{III}(bpy)_3](PF_6)_3$ EPR data are from ref 33. [b] Error limits on k and ν/ξ values are intended to represent value ranges obtained from calculations for the given g value error limits.

Shoulders on the latter band occur at 440 and 520 nm.

The logarithms of the diffuse-reflectance remission functions may be considered as directly proportional to the logarithms of the concentrations of absorbing species at individual wavelengths for these materials.[30] Hence it is possible to obtain an estimate of the efficiency of the Ru(II) oxidation reaction. If $[Ru^{II}(bpy)_3]^{2+}$ was the only absorber at 450 nm, an 85% loss in [Ru(II)] is calculated. We judge 85% conversion as a lower limit, however, since the product, $[Ru^{III}(bpy)_3]^{3+}$, is also known to absorb at 450 nm.[31] A better estimate of 92% conversion is obtained if absorption coefficients of 14000 (λ_{450}), ca. 70 (λ_{685}) and 500 (λ_{450}), 420 (λ_{685}) M^{-1} cm^{-1} for the Ru(II) and Ru(III) complexes, respectively, are assumed applicable in the zeolite. The three large absorption coefficients are literature values.[3,31] The ±70 (λ_{685}) value was estimated from the difference in apparent absorbances at 685 nm between the spectra of curves a and b in Figure 1.

Longer chlorine exposure times did not increase the Ru(III) yield for the 2.1 wt % Ru sample. Certain complexes may reside in locations that make them difficult to oxidize. These locations might occur when the six large cavities surrounding a given complex also contain complexes. In this case the chlorine molecule or atom (diameter ~0.199 nm[32]) may be unable to diffuse to the isolated Ru(II) center or, more likely, oxidation would not proceed because there would be no room to accommodate the product chloride ion (diameter ~0.362 nm[32]). At a 2.1 wt % Ru loading, with the assumption of 100% initial Ru(II) complex formation, about 44% of the supercages in a Y zeolite would contain complexes. On the basis of the argument above, higher complex loadings should increase the number of unoxidizable sites. In fact, prolonged chlorine exposure to samples manifesting 65% and 87% supercage occupancy resulted in Ru(III) yields of only 20% and <5%, respectively. As a consequence, further study of the material with the highest loading was discontinued.

(28) Pedersen, L. A.; Lunsford, J. H. *J. Catal.* **1980**, *61*, 39. Lunsford, J. H.; Treybig, D. S. *Ibid.* **1981**, *68*, 192. Gustafson, B. L.; Lunsford, J. H. submitted for publication in *J. Catal.*
(29) Miller, R. R.; Brandt, W. W.; Puke, M. *J. Am. Chem. Soc.* **1955**, *77*, 3178.
(30) Delgass, W. N.; Haller, G. L.; Kellerman, R.; Lunsford, J. H. "Spectroscopy in Heterogeneous Catalysis"; Academic Press: New York, 1979; p 101.
(31) Demas, J. N.; Adamson, A. W. *J. Am. Chem. Soc.* **1973**, *95*, 5159.
(32) Weast, R. C., Ed. "Handbook of Chemistry and Physics"; The Chemical Rubber Co.: Cleveland, 1970; pp F152–F155.

The electron paramagnetic resonance (EPR) spectrum of the degassed, 2.1 wt % Ru, $[Ru^{III}(bpy)_3]$–Y sample is reproduced in curve a of Figure 3. The experimentally determined $g_\perp$ and $g_\parallel$ values for the zeolite-supported low-spin d^5 complex are presented in Table III for comparison with DeSimone and Drago's[33] values for $[Ru^{III}(bpy)_3](PF_6)_3$ doped in a powdered, diamagnetic host. The weak, broad $g_\parallel$ absorption is readily observable at higher receiver gain, curve b of Figure 3, and its field position was reproducible from sample to sample. The previous authors[33] noted that the value of $g_\parallel$ was sensitive both to changes in the type of host material and to changes in complex concentration within the host. Although the nature of the dependence of the $g_\parallel$ value on these changes was not discussed, it is reasonable that our $g_\parallel$ value differs significantly from theirs since the environment within the anionic zeolite lattice is undoubtedly at variance with their host matrix. However, our $g_\parallel$ value is still well within their computed range of possible values.

Larger values of the trigonal field splitting parameter[33] (ν/ξ) and the orbital reduction factor[33] (k) were calculated for $[Ru^{III}(bpy)_3]$–Y than for $[Ru^{III}(bpy)_3](PF_6)_3$, as shown in Table III. Although evaluation of k with respect to the degree of d-electron delocalization of the ligand is tenuous, increasing values of k should reflect decreasing metal–ligand covalency within a related class of complexes for a particular metal ion. In congruence, complexes of identical composition that exhibit different k values probably experience varying degrees of environmental perturbation sufficient to induce changes in orbital splittings. It is possible that the $[Ru^{III}(bpy)_3]^{3+}$ ion within the zeolite supercage encounters higher negative charge density or suffers greater axial distortion as a result of structural lattice compression on the complex than it does in the doped powder sample.

$[Ru^{III}(bpy)_3]$–Y + H_2O. Light green, 2.1 wt % Ru, $[Ru^{III}(bpy)_3]$–Y turned orange, indicative of reduction to $[Ru^{II}(bpy)_3]$–Y, upon exposure to vapor or liquid phase water. Most of the reactions were conducted in small-diameter Pyrex tubes, and at room temperature the water appeared to absorb preferentially near the top of the zeolite bed since the color change was observed to move slowly but progressively down the bed. It was found that heating the Ru(III) sample to 70 °C produced a faster reaction. The heat treatment was probably necessary to stimulate water desorption and enhance its mobility within the zeolite. In this context, when a tube containing 2.1 wt % Ru, $[Ru^{III}(bpy)_3]$–Y, was opened and the sample immersed immediately in a beaker of water at 25 °C, rapid (<1 min) and complete change of color occurred throughout the sample. Effervescence, which might have been an indication of O_2 evolution, was not observed.

Water was condensed directly onto 2.1 wt % $[Ru^{III}(bpy)_3]$–Y, and following an exposure time of 15 h at 70 °C and subsequent outgassing at 25 °C for 6 h, a visible-region diffuse-reflectance spectrum was recorded, as displayed in curve c of Figure 1. Growth in intensity of the 450-nm band coincided with a marked loss in intensity of the band at 685 nm. If $[Ru^{II}(bpy)_3]^{2+}$ is considered the only absorber at 450 nm and $[Ru^{III}(bpy)_3]^{3+}$ the only absorber at 685 nm, then an 83% loss in Ru(III) is calculated on the basis of changes in log ($F(R_\infty)$) values from curve b to curve c of Figure 1, at 685 nm. A concomitant 78% gain in Ru(II) is calculated from the 450-nm changes. An 89% increase in Ru(II), with a corresponding Ru(III) decrease of 88%, is obtained from calculations that incorporate appropriate extinction coefficients and assume that both oxidation states absorb at both wavelengths. Repeated experiments under different conditions resulted in no significant improvement over the apparent 90% reduction of Ru(III) on the basis of diffuse-reflectance measurements.

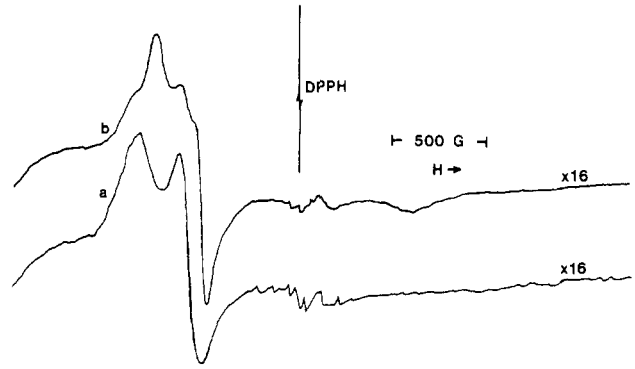

Figure 4. Electron paramagnetic resonance spectra taken at −196 °C: (a) same as Figure 3c, but at 16× greater receiver gain; (b) sample of part a after degassing at 130 °C.

EPR spectra were obtained for comparison. The EPR spectrum displayed in curve c of Figure 3 was taken shortly after obtaining the diffuse-reflectance spectrum of Figure 1c. In agreement with the diffuse-reflectance results, greater than 88% loss of the total number of Ru(III) spins following the reaction was calculated on the basis of comparison of the areas, obtained by double integration, of curves a and c in Figure 3. However, distortion of the residual Ru(III) signal in Figure 3c is evident. The spectrum is displayed at higher gain in Figure 4a. Degassing the sample further at 130 °C for 24 h resulted in further distortion of the Ru(III) EPR signal, as seen in Figure 4b. These EPR results will be discussed below.

Analyses of the gases above the samples following reactions were made by using gas chromatography and mass spectrometry. Dioxygen was never detected as a product;[34] however, some carbon dioxide corresponding to an amount equivalent to about 6% of the total ruthenium was always observed. If oxygen-18-labeled water was used, oxygen-18 was incorporated in the CO_2 as evidenced by intensity ratios of ~4:4:1 for m/e values 48, 46, and 44 in the mass spectrum. Therefore, water is undoubtedly the source of oxygen in the CO_2. At this time we have no satisfactory hypothesis for the origin of the carbon, but CO_2 is definitely produced from the reaction since both the water and the zeolite were outgassed, and tested free of CO_2, prior to the reaction. We note that CO_2 evolution has been observed before in photosystems that contain $[Ru^{II}(bpy)_3]^{2+}$ and EDTA.[8] The oxidation of organic impurities containing carboxyl or hydroxyl groups by hydroxyl radicals produced from water oxidation in the zeolite is a possibility.

The inability of $[Ru^{III}(bpy)_3]$–Y to produce dioxygen from water might be better understood by considering the behavior of the complexes in aqueous solution. On the basis of the kinetics for the reactions of $[Ru^{III}(bpy)_3]^{3+}$ with water, hydroxide ion, and hydrogen peroxide, Creutz and Sutin[3] proposed mechanisms for dioxygen formation from the reaction of $[Ru^{III}(bpy)_3]^{3+}$ with water. In rather simplified form the first mechanism involves eq 6 and 7, followed by steps in which

$$[Ru^{III}(bpy)_3]^{3+} + H_2O \xrightarrow{\text{slow}} [Ru^{II}(bpy)_3OH]^{2+} + H^+ \quad (6)$$

$$[Ru^{II}(bpy)_3OH]^{2+} + [Ru^{III}(bpy)_3]^{3+} \rightarrow [Ru^{III}(bpy)_3OH]^{3+} + [Ru^{II}(bpy)_3]^{2+} \quad (7)$$

a proton is lost from the bound hydroxyl and H_2O_2 is formed on contact of the oxy-bound Ru(III) complex with water. Peroxide oxidation to O_2 would follow from electron transfer to an additional 2 equiv of Ru(III) complex. [Ru^{II}-

(33) DeSimone, R. E.; Drago, R. S. *J. Am. Chem. Soc.* **1970**, *92*, 2343.

(34) Dioxygen production corresponding to ≥1% $[Ru^{III}(bpy)_3]^{3+}$ reduction should have been detected easily under our conditions.

$(bpy)_3OH]^{2+}$ in eq 6 suggests that the hydroxyl radical, initially formed from direct attack of OH^- on $[Ru^{III}(bpy)_3]^{3+}$, would not be dissociated from the complex. Others[35] have also proposed that the $[Ru^{II}(bpy)_3OH]^{2+}$ intermediate would contain a covalently hydrated bipyridine ligand such as that resulting from eq 8. Equation 7 presumes an excess of

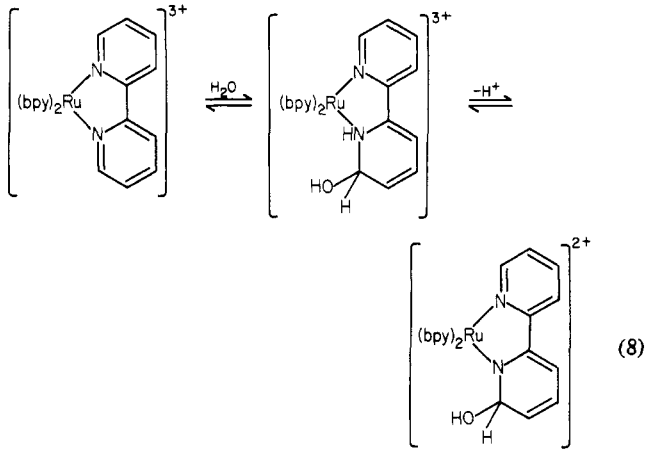

(8)

$[Ru^{III}(bpy)_3]^{3+}$. Peroxide would decompose slowly to give O_2 and H_2O, but in the presence of excess $[Ru^{III}(bpy)_3]^{3+}$, more rapid peroxide oxidation would be possible.

Creutz and Sutin[3] postulated that the mechanism above might be partly responsible for O_2 formation above pH 7 and predominate above pH 13. Below pH 13 and predominately below pH 7, a second mechanism was invoked in which peroxide is not a dioxygen precursor. In this second mechanism 2 equiv of eq 6 and 7 would begin the sequence, followed by loss of a proton from the bound hydroxyl. Then O_2 would form via eq 9. The authors[3] observed a maximum dioxygen yield

$$[Ru^{III}(bpy)_3OH]^{3+} + [Ru^{III}(bpy)_3O]^{2+} \rightarrow 2[Ru^{II}(bpy)_3]^{2+} + O_2 + H^+ \quad (9)$$

at pH 9. They emphasized that their schemes were certainly not the only ones possible, but two of their main points might bear on our work. First, the hydroxyl radical initially formed would remain bound to the ruthenium complex during the oxidation process since free hydroxyl radical formation should be very unfavorable thermodynamically. Second, once formed, immediate reaction of the bound hydroxyl radical with another $[Ru^{III}(bpy)_3]^{3+}$ ion would result in dioxygen formation only if the Ru(III) concentration is high; i.e., Ru(III) should be readily available for reaction.

We note that the large ruthenium complexes are effectively immobilized within the zeolite; i.e., they cannot move to make contact with other complexes. The closest metal–metal separation would be about 1.24 nm on the basis of typical unit cell constants,[26] leaving a space of about 0.16 nm between complexes on the basis of a complex diameter of 1.08 nm.[25] With the assumption that the zeolite lattice was not interposed between them, this intercomplex distance should be close enough for electron transfer from a bound hydroxyl complex to a second Ru(III) complex. Although higher loadings would increase the number of close contact complexes, our inability to form sufficiently high concentrations of Ru(III) by chlorine oxidation precluded adequate evaluation of those systems. (The 3 wt % Ru sample, 20% oxidized to $[Ru^{III}(bpy)_3]$–Y, was exposed to water and reduction of Ru(III) to Ru(II) did occur but no O_2 was detected.) Even though the complexes might lie close enough to one another, it is possible that the zeolite orients them within the supercages in a manner that would preclude efficient electron transfer between them. In that case, water would effect the reduction of individual complexes but further intercomplex oxidation of covalently bound hydroxyls would not occur.

In contrast to Creutz and Sutin's proposed mechanisms for the ruthenium(III) system, Nord and Wernberg[36] proposed a mechanism for the reduction of $[Fe^{III}(bpy)_3]^{3+}$ by hydroxide ion that did not involve intercomplex electron transfer. Instead, they invoked the participation of free hydroxyl radicals in the electron-transfer or hydroperoxide-forming steps. In our case, mobile hydroxyl radicals within the zeolite should have formed hydroperoxide rather readily, unless they were trapped by another agent. A suitable trapping agent might have been free bipyridine, which could not be washed completely from the support. It is known that hydroxyl radicals will attack heterocycles such as pyridine with formation of phenolic type compounds.[37] For example, 3-hydroxypyridine would be one of the products if pyridine were the precursor, especially in the presence of oxidizing agents. However, we do not feel that this possibility deserves much consideration since Nord and Wernberg[36] observed that the addition of free ligand to the $[Fe^{III}(bpy)_3]^{3+}$ system did not affect the rate of dioxygen production.

One should not overlook the observed importance of conducting the reaction in the proper pH range. Creutz and Sutin noted that the maximum O_2 yield occurred at pH 9.[3] In repeating that work, Shafirovich, Khannanov, and Strelets also noted the marked drop in O_2 production below pH 7 and above pH 11.[14] In fact, no O_2 was observed outside of the pH 6–12 range. Although zeolites often exhibit basic behavior in aqueous solution, it is difficult to estimate the "effective" pH within the $[Ru^{III}(bpy)_3]$–Y zeolite. It may well fall within an undesirable range.

Certain transition-metal hydroxo complexes and oxides serve as catalysts for solution-phase O_2 formation from the reaction between $[Ru^{III}(bpy)_3]^{3+}$ and water.[4,5,13-17] In even more marked contrast to the mechanisms discussed above, it is believed that in these systems the redox catalysts assume the task of hydroxyl-radical carrier, rather than the ruthenium tris(bipyridine) complex. As an example, the behavior of a cobalt(II) hydroxy complex–$[Ru^{III}(bpy)_3]^{3+}$ system was described[14] by a mechanism in which steps involving electron transfer from the cobalt hydroxy complexes to the Ru(III) complex alternate with steps involving hydroxide attack on the cobalt centers. Hydroxide attack on a $[Co^{IV}(OH)_2]^{2+}$ moiety would produce H_2O_2, which could be oxidized to O_2 with an additional 2 equiv of Ru(III) complex. In this system the overall dioxygen yield depended not only on the pH conditions but also on the relative ratio of redox catalyst centers to Ru(III) centers. The O_2 yields in the redox catalyst–$[Ru^{III}(bpy)_3]^{3+}$ systems are much higher than those observed for the simpler aqueous $[Ru^{III}(bpy)_3]^{3+}$ system, regardless of the pH. In fact, Shafirovich et al. have suggested[14] that it is impurities such as iron ions in the Creutz and Sutin[3] system that catalyze O_2 production, implying that the covalently hydrated tris(bipyridine)ruthenium(III) complex mechanism is unimportant for O_2 production.

Although both Fe(III) and Mn(II) were present as impurities in our samples and hydroxo complexes of these ions are effective as catalysts in solution,[14] they were apparently ineffective in our system. In a related study, RuO_2 was formed on the external surfaces of a Y zeolite and $[Ru^{III}(bpy)_3]^{3+}$ was then synthesized within it.[38] The loading levels of both the

(35) Arce Sagüés, J. A.; Gillard, R. D.; Lancashire, R. J.; Williams, P. A. *J. Chem. Soc., Dalton Trans.* **1979**, 193.

(36) Nord, G.; Wernberg, O. *J. Chem. Soc., Dalton Trans.* **1972**, 866.

(37) Selvarajan, N.; Raghavan, N. V. *J. Phys. Chem.* **1980**, *84*, 2548.

oxide and the complex were 1 wt % Ru. Again no O_2 was detected on exposure of this material to H_2O. Undoubtedly the redox catalysts require close contact with the Ru(III) complex to transfer electrons efficiently, and perhaps the complexes require more mobility than they are afforded within the zeolite supercages to interact with catalyst sites. Again, it is difficult to ascertain whether the zeolite provides an appropriate "effective" pH range for O_2 production via redox catalysis. Lehn, Sauvage, and Ziessel[17] supported RuO_2 on Y zeolites and did observe a pH dependence on O_2 yield. However, in their study the tris(bipyridine)ruthenium(III) complexes were in solution phase, rather than immobilized within the zeolites.

Very little can be said regarding the residual EPR spectra in Figure 4 at this point since the composition of the remaining material is unknown, although these spectra are apparently due to Ru(III) complexes. The lines near $g = 2.00$ do not change appreciably during the course of the reaction and are due to Mn(II) impurities as well as other radicals present in the sample prior to the reaction of interest. We find no evidence for O_2^- or OH· in the spectra, nor do we see evidence for free hydroxy–bipyridyl radicals. The residual Ru(III) signal in Figure 4a does resemble in shape, if not in exact g values, the spectrum of $[Ru^{III}(bpy)_3H_2O]^{3+}$, a compound postulated as a covalent hydrate[35] in which the water molecule is pictured as added across one of the C–N double bonds of a bpy ligand (eq 8). Again, structures similar to this were also proposed by Creutz and Sutin for the nondissociated hydroxyl radical in eq 6–9 of this paper.[3] It is possible then that Figure 4a is the spectrum of a trapped reaction intermediate. Figure 4b would then appear to be the spectrum of a mixture of that complex with another unknown complex, perhaps a decomposition product such as $[Ru^{III}(bpy)_2]X_2$. We should note that Shafirovich et al.[14] have suggested that the nonquantitative yields of O_2, based on the amount of oxidants in their systems, probably arise from competitive reactions that result in bpy ligand oxidation. They calculated that oxidation of 2–3% of the aromatic bpy rings would be adequate for complete reduction of $[Ru^{III}(bpy)_3]^{3+}$. This susceptibility of the bpy complexes to decomposition may make them unsuitable for long-term use as reactants or photocatalysts for photochemical water-splitting applications.

Conclusion

The XRD and XPS studies confirm that $[Ru^{II}(bpy)_3]^{2+}$ complexes may be synthesized within the large cavities of a Y type zeolite. Chlorine gas may be used effectively for preparing $[Ru^{III}(bpy)_3]$–Y from the divalent material, but attempts to explore the higher oxidation states of other large transition-metal complexes in zeolites, through oxidation of lower valent analogues by chlorine gas, should be done at complex loadings of less than 50% of the supercage capacity.

The zeolite lattice offered the $[Ru^{III}(bpy)_3]^{3+}$ ion an environment quite different from that of a complex salt matrix, as shown by the EPR study. Reduction of $[Ru^{III}(bpy)_3]^{3+}$ ions by water is possible in a Y zeolite, just as in aqueous solution. However, if O_2 production is desired from a catalytic or photocatalytic process in which $[Ru^{III}(bpy)_3]^{3+}$ ions are intended as water oxidizing agents, immobilization of the complexes within zeolite lattices would appear to be self-defeating. Although the mechanistic aspects are still uncertain, it would be more desirable to maintain the tris(bipyridine)ruthenium complexes in solution. There they would experience greater mobility, and better control of their immediate environment (i.e., pH) could be achieved. On the other hand, immobilization of $[Ru^{III}(bpy)_3]^{3+}$ ions may be attractive if water oxidation intermediates such as hydroxyl radicals are desired for other purposes such as oxidizing organic substrates. The integrity of the complexes during these oxidation processes may pose a serious problem, however, since certain reactions appear to result in complex decomposition.

Experimental Section

Materials. The Y zeolite was from Linde, Lot No. 3365-94, lot analysis SiO_2 65.5% and Al_2O_3 22.2%. Synthesized and impregnated $[Ru^{II}(bpy)_3]$–Y samples were prepared by the method described in ref 1 except that a 3.5:1 mole ratio of 2,2′-bipyridine to ruthenium was used rather than a 4:1 ratio for the synthesized samples. High-purity chlorine was obtained from Matheson.

Complex Location. XRD patterns were recorded with a Seifert-Scintag PAD II diffractometer using Ni-filtered Cu radiation. XPS was done with a Hewlett-Packard Model 5950A spectrometer using monochromatic Al K_α X radiation (1486.6 eV) and a window width of 20 eV at analyzing chamber pressures less than 4×10^{-9} torr. Samples were pressed into thin wafers and then outgassed to less than 2×10^{-5} torr at 100 °C prior to introduction in the XPS spectrometer. Sample charge compensation was achieved with an electron-flood gun. The absolute binding energy values are not strictly reliable since these materials are insulators. For comparison purposes, a binding energy of 154.0 eV was arbitrarily assigned to the Si 2s peak. An average C 1s value of 285.7 eV for the zeolite samples was used to normalize the binding energies of the crystalline $[Ru^{II}(bpy)_3]Cl_2 \cdot xH_2O$ sample. XPS peak areas (I_x) were corrected by normalization to 80 scans, and then element concentration ratios (n_1/n_2) were calculated by using Scofield's[39] photoelectron cross sections (σ_x); $n_1/n_2 = I_1\sigma_2/I_2\sigma_1$.

$[Ru^{III}(bpy)_3]$–Y. Samples of 2.1 wt % Ru, synthesized $[Ru^{II}(bpy)_3]$–Y, previously degassed at 200 °C for 24 h, were exposed at 65 °C to between 500 and 700 torr of chlorine gas for 2–14 h. The light green samples were then degassed, usually at 65 °C for 2 h prior to further study. Lower reaction temperatures resulted in only slightly lower conversions to $[Ru^{III}(bpy)_3]$–Y. Reaction temperatures higher than 80 °C produced brown-green samples, which were shown to contain $[Ru^{III}(bpy)_3]^{3+}$ by EPR analysis, but because of the discoloration these samples were not studied further. Reaction times longer than 3 h did not substantially increase the $[Ru^{III}(bpy)_3]$–Y yield. Chlorine exposure times for 3 and 4 wt % Ru, $[Ru^{II}(bpy)_3]$–Y samples were 26 and 259 h, respectively.

Reactions were conducted in sample tubes equipped with 0.5-cm fused-quartz cuvettes for diffuse-reflectance studies and 4-mm o.d. Pyrex side arms for EPR studies. Gas-sampling tubes were connected to the sample tubes for use in mass spectrometric work. For gas chromatographic analysis, sample tubes were connected directly to a gas-sampling loop. Water was degassed by standard vacuum-line techniques just prior to exposure to the samples.

Spectroscopic Methods. Visible-region (320–800 nm) diffuse-reflectance spectra were recorded with a Cary 14 spectrophotometer equipped with a Type II diffuse-reflectance attachment. The logarithms of the Schuster–Kubelka–Munk remission functions were calculated by $\log (F(R_\infty)) = \log [(1 - 10^{-A'})^2/(2 \times 10^{-A'})]$, where $A' = (A_{sample} - A_{ref})$, and A, the apparent absorbance obtained directly from the spectrometer, is directly related to the reflectance (R_∞) by $\log R_\infty = -A$. Absorber concentrations (C) and extinction coefficients (α) are related to $\log (F(R_\infty))$ values at given wavelengths by $\log (F(R_\infty)) = \log C + \log \alpha + \text{constant}$.

X-Band EPR spectra were obtained with a Varian E6S spectrometer at −196 °C. The g values were calculated relative to a DPPH standard. For comparison with literature results,[33] values of k and ν/ξ were calculated from the equations of Bleany and O'Brien,[40] where $g_{\parallel} = 2[\sin^2\theta - (1 + k)\cos^2\lambda]$, $g_{\perp} = -2[2^{1/2}k \cos\theta \sin\theta + \sin^2\theta]$, $\tan 2\theta = 2^{1/2}(0.5 - \nu/\xi)$, and $0 < 2\theta < \pi$.

Mass spectrometric measurements were performed with a CEC 21-614 residual gas analyzer. A Gow-Mac Model 10-285 thermal conductivity cell was used for gas chromatographic analyses. A glass

(38) Quayle, W. H.; Lunsford, J. H., unpublished results. Zeolite-supported RuO_2 was prepared in a manner similar to that reported by Lehn et al.,[17] except that $Ru(NH_3)_6X_3$ salts were used rather than $RuCl_3 \cdot xH_2O$. Also, pure O_2, instead of air, was used for the oxidation, which was conducted at 265 °C for 14 h. $[Ru^{III}(bpy)_3]^{3+}$ was synthesized within this material by following the method described in the Experimental Section of this paper.

(39) Scofield, J. H. *J. Electron Spectrosc. Relat. Phenom.* **1976**, *8*, 129.
(40) Bleany, B.; O'Brien, M. C. M. *Proc. Phys. Soc., London, Sect. B* **1956**, *69*, 1215.

sampling loop attached to a high-vacuum manifold was used in conjunction with a 2 m × $^1/_8$ in. SS Porapak Q column followed by a 1 m × $^1/_8$ in. SS Molecular Sieve 5A column. A Carle Model 5521 switching valve was situated between the columns. Valve switching during analyses avoided contamination of the zeolite column by CO_2 or H_2O.

Acknowledgment. The financial support of this work through NSF Grant CHE-7706792 is gratefully acknowledged.

Registry No. $[Ru^{III}(bpy)_3]^{3+}$, 18955-01-6; $[Ru^{II}(bpy)_3]^{2+}$, 15158-62-0; $[Ru^{II}(bpy)_3]Cl_2$, 14323-06-9.

Contribution from the Department of Chemistry and the Materials and Molecular Research Division, Lawrence Berkeley Laboratory, University of California, Berkeley, California 94720

Equilibrium Constant for the Dimerization of Bisulfite Ion To Form $S_2O_5^{2-}$

ROBERT E. CONNICK,*[1] THOMAS M. TAM, and ECKART VON DEUSTER

Received February 25, 1981

At high concentrations in aqueous solution, bisulfite ion dimerizes to form the species $S_2O_5^{2-}$. The equilibrium quotient for the reaction $2HSO_3^- \rightleftharpoons S_2O_5^{2-} + H_2O$ has been determined by combining Raman intensity measurements of HSO_3^- with ultraviolet absorption data on $S_2O_5^{2-}$. Unlike previous determinations, the method requires no assumption about constancy of the equilibrium quotient over the range of solutions measured, although it was necessary to assume a constant molar absorptivity in the UV for $S_2O_5^{2-}$ and a constant molar Raman intensity for HSO_3^-. Earlier measurements reported in the literature, based only on UV measurements of $S_2O_5^{2-}$ absorption and the assumption of constant equilibrium quotient and molar absorptivity, are shown to be seriously in error. Variations of the equilibrium quotient with ionic strength and temperature are reported. A value of Q_d of 0.088 M^{-1} was found for a dilute solution of bisulfite in 1 M $NaClO_4$ solution at 25 °C. In addition to the well-characterized form of bisulfite ion having the hydrogen attached to the sulfur, Raman evidence is reported for the presence of appreciable amounts of the isomer with the hydrogen bonded to one of the oxygens.

In aqueous solutions of bisulfite ion, the following dimerization equilibrium is established rapidly:

$$2HSO_3^- \rightleftharpoons S_2O_5^{2-} + H_2O \quad Q_d = [S_2O_5^{2-}]/[HSO_3^-]^2$$

Although several investigators[2,3] have attempted to measure Q_d, the results are far from concordant, as shown in Table I, and an examination of the method used indicates that none of the values of Q_d is reliable.

All previous investigators measured the ultraviolet absorption of $S_2O_5^{2-}$ in a region where HSO_3^- absorbs negligibly. The value of Q_d was obtained by a simultaneous fitting of the data with two parameters, assumed to be constant: Q_d and a_d, the molar absorptivity of $S_2O_5^{2-}$. To obtain reliable values for these parameters, it is necessary to convert an appreciable fraction of the total bisulfite to the dimer at the highest concentration studied. A reexamination of Golding's[2a] data shows no evidence of appreciable conversion. Arkhipova and Chistyakova[2b] investigated such a small concentration range that their results could give no meaningful information on fraction conversion. Bourne et al.[3] made a careful study at constant ionic strength and applied corrections for the presence of SO_2 and SO_3^{2-}. At their highest bisulfite concentration, 0.160 M, their interpretation of the data yielded 5% conversion to the disulfite dimer. But a 5% drift in Q_d could have equally well accounted for the data. Because Q_d is small, it is necessary to increase the bisulfite concentration to rather large values to produce appreciable conversion to the dimer. In doing so, the composition of the solution must be changed significantly, and consequently it is not safe to assume that Q_d will remain constant. Therefore in redetermining Q_d a method was sought which would not require the assumption of constant Q_d over the range of solution composition studied.

In the course of the study, information was obtained on the structure of bisulfite ion in solution. Evidence is presented that both isomeric forms of bisulfite, i.e., with the proton attached to the sulfur and with the proton attached to an oxygen, are present in solution in appreciable amounts.

Table I. Literature Values of the Equilibrium Quotient Q_d for the Reaction $2HSO_3^- \rightleftarrows S_2O_5^{2-} + H_2O$

temp, °C	ionic strength, M	$a_{S_2O_5^{2-}}$ (wavelength, nm)	Q_d, M	investigator
20	0.07-0.32	4×10^3 (255)	0.07	Golding[2a]
22	0.18	142.9 (258)	2.0	Arkhipova and Chistyakova[2b]
25.0	2.0	1980 (255)	0.34	Bourne, Higuchi, and Pitman[3]
	0	1980 (255)	0.076	

Method

It would be desirable to have a physical measurement which would detect directly the concentration of bisulfite ion in the equilibrated solution. Unfortunately absorption spectra measurements will not do this, because $S_2O_5^{2-}$ absorbs appreciably at all wavelengths where bisulfite ion absorbs, and there is no independent way of obtaining the molar absorptivity of $S_2O_5^{2-}$. Instead, the Raman emissivity of bisulfite ion was determined quantitatively from the intensity of the Raman line of the H-S stretch at 2532 cm^{-1}. At the same time, the ultraviolet absorption spectrum of the equilibrated solutions was also measured at 320 nm, a wavelength at which $S_2O_5^{2-}$ absorbs strongly and the absorption of bisulfite ion is negligible. These data were then combined to give values of Q_d.

The Raman intensity, I, of the 2532-cm^{-1} band should be directly proportional to the concentration of bisulfite ion:[4]

$$I = i[HSO_3^-] \quad (1)$$

with the proportionality constant i, the molar Raman intensity, unknown. The intensity divided by the total bisulfite, where

$$[\sum HSO_3^-] = [HSO_3^-] + 2[S_2O_5^{2-}] \quad (2)$$

(1) To whom correspondence should be addressed at the Department of Chemistry.
(2) (a) R. M. Golding, *J. Chem. Soc.*, 3711 (1960); (b) G. P. Arkhipova and I. I. Chistyakova, *Zh. Prikl. Khim. (Leningrad)*, **44**, 2193 (1971).
(3) D. W. A. Bourne, T. Higuchi, and I. H. Pitman, *J. Pharm. Sci.*, **63**, 865 (1974).
(4) For convenience, the symbol HSO_3^- will be used to represent the sum of the concentrations of the two isomers.

0020-1669/82/1321-0103$01.25/0